1H-Nuclear Magnetic Resonance-Based Plasma Metabolic Profiling of Dairy Cows with Fatty Liver

Chuang Xu[a],*, Ling-wei Sun[1,a], Cheng Xia, Hong-you Zhang, Jia-san Zheng, and Jun-song Wang[2]

Department of Clinical Veterinary Medicine, Animal Science and Technology College,
Heilongjiang August First Land Reclamation University, Daqing 163319, China

ABSTRACT: Fatty liver is a common metabolic disorder of dairy cows during the transition period. Historically, the diagnosis of fatty liver has involved liver biopsy, biochemical or histological examination of liver specimens, and ultrasonographic imaging of the liver. However, more convenient and noninvasive methods would be beneficial for the diagnosis of fatty liver in dairy cows. The plasma metabolic profiles of dairy cows with fatty liver and normal (control) cows were investigated to identify new biomarkers using 1H nuclear magnetic resonance. Compared with the control group, the primary differences in the fatty liver group included increases in β-hydroxybutyric acid, acetone, glycine, valine, trimethylamine-*N*-oxide, citrulline, and isobutyrate, and decreases in alanine, asparagine, glucose, γ-aminobutyric acid glycerol, and creatinine. This analysis revealed a global profile of endogenous metabolites, which may present potential biomarkers for the diagnosis of fatty liver in dairy cows. (**Key Words:** Dairy Cow, Fatty Liver, 1H-Nuclear Magnetic Resonance, Metabolomics, Plasma)

INTRODUCTION

Fatty liver is a common metabolic disorder in dairy cows during the transition period. Up to 65% of dairy cows are affected by moderate (triacylglycerol [TAG] 50 to 100 mg/g of wet liver) or severe (TAG ≥100 mg/g of wet liver) fatty liver during early lactation (Jorritsma et al., 2000). The primary pathological feature of fatty liver is the excessive deposition of fat, which predominantly consists of TAG, in the liver. Most transition dairy cows are in a state of negative energy balance (NEB) due to increased energy demands after parturition, coupled with lagging dry matter intake (DMI) (Hayirli et al., 2002). The most direct factor in the induction of fatty liver is a NEB (Oikawa et al., 2010). The economic results of fatty liver are reduced milk yield (MY), poor fertility, high risks of other periparturient diseases, and early culling of affected animals. As fatty liver can lead to substantial economic losses in the dairy industry, its prevention is of the utmost importance.

Several risk factors have been suggested, which include a high body condition score caused by prolonged lactation because of reproductive failure and overfeeding in late lactation and the dry period, a high rate of body lipid mobilization around calving, a low feed intake, and a low protein content in the diet (Sejersen et al., 2012). However, there is no consensus regarding the overall metabolic state for fatty liver in dairy cows. Many new holistic metabolomic platforms have been used for the identification of new predictive markers for the early diagnosis of this disease.

At present, the diagnosis of fatty liver has been restricted to biochemical or histological examinations of liver biopsy specimens (Gonzalez et al., 2011). Biopsy of the liver is the most reliable method for accurate estimation

* Corresponding Author: Chuang Xu. Tel: +86-459-6819121, Fax: +86-459-6819121, E-mail: xuchuang7175@gmail.com
[1] Jiangsu Engineering Technology Research Center of Meat Sheep & Goat Industry, Nanjing Agricultural University, Nanjing, 210095, China.
[2] Center for Molecular Metabolism, School of Environmental and Biological Engineering, Nanjing University of Science Technology, Nanjing, 210095, China.
[a] These two authors contributed equally to this work.

of the degree of fatty infiltration. It can be used to determine the concentration of triglycerides (TGs) and the severity of the fatty liver (Herdt et al., 1983). For on-farm testing, liver biopsies are impractical due to the injury to the animals and the time needed to acquire and analyze the samples. Biopsy causes decreased feed intake and increased danger of infection and hemorrhage in cows (Smith et al., 1997). Furthermore, liver biopsy has been found to induce behavioral changes for up to 19 h afterwards; particularly for behavior previously associated with pain. Ultrasonographic imaging of the liver is a recently developed, noninvasive method; however, it requires skilled operating experience and is costly.

Due to the rapid development of metabolomics in recent years, the use of this approach for disease biomarker assessment has become popular. As the preferred platform of the metabolomics technologies, ^{1}H nuclear magnetic resonance (NMR) can provide a comprehensive metabolic profile of proton-containing, low-molecular-weight metabolites, and requires a minimal amount of sample (Song et al., 2013). The objective of the current study was to use ^{1}H NMR-based plasma metabolomics to examine fatty liver in dairy cattle to obtain information for understanding the metabolic pathways, metabolic networks, and pathogenesis of the fatty liver.

MATERIALS AND METHODS

Ethics statement

This study was carried out in strict accordance with the recommendations in the Guide for the Care and Use of Laboratory Animals of the National Institutes of Health. The protocol was approved by the Committee on the Ethics of Animal Experiments of the Heilongjiang Bayi Agricultural University (Permit Number: 20120319-1). All surgery was performed under sodium pentobarbital anesthesia, and all efforts were made to minimize suffering.

Animals

After obtaining the owner's permission, blood and tissue samples from cows were collected from a commercial dairy farm located in Heilongjiang Province, China. All samples—from 171 Holstein cows (14 to 21 days after calving)—were collected prior to feeding in the morning. The samples were collected from March 2014 to September 2014.

For this experiment, the cows were fed a total mixed ration (TMR) at 0070, 1300, and 1900 h. The TMR consisted of 55.60% dry matter (DM), 16.40% crude protein, 5.60% fat, 34.30% neutral detergent fiber, 22.00% acid detergent fiber, 1.07% calcium, 0.49% phosphorus, 0.32% magnesium, 0.13% sodium, 1.40% potassium,

0.39% chloride, 0.22% sulfur, and 1.75 mcal/kg DM net energy for lactation (Zhang et al., 2013).

The data collected during examination of the cows included age, parity, postpartum days, MY, body condition score (BCS), and DMI. The BCS (5-point scale) of 1 (thin) to 5 (obese) points with 0.25 intervals is used to assess body fat stores, and describes the appearance of seven body regions in Holstein dairy cows (Wildman et al., 1982). The MY of cows in this experiment was recorded using the calibrated weigh jars in the milking parlor on the same day *as* the collection of the blood samples. Individual feed intake was measured daily. Samples of feeds and TMR were collected weekly and dried at 60°C for 72 h. The DM percentages of the feed ingredients were used to adjust ration components each week, and DM percentages of TMR were used to calculate daily DMI.

Sample collection

The tissue and blood liver samples obtained from the experimental cows were collected on the same day. The blood samples were obtained from the jugular vein, stabilized in sodium heparin, and immediately centrifuged at 1,400×*g* for 20 min at 4°C. The plasma samples obtained were subsequently stored at –80°C until further analysis. Liver transfixion pins were used for the collection of liver tissue samples from the 11th or 12th right intercostal space. Ten milliliters of procaine 2% (CDM Lavoisier, Paris, France) was used to anaesthetize the skin around the 12th intercostal space. Liver tissue samples were collected with tailor-made biopsy needles (Berlin Model, 2.5 mm×25 cm; Eickemeyer Medizintechnik für Tierärzte, Tuttlingen, Germany), and biopsy specimens (150 to 350 mg of liver tissue) were stored at –20°C until determination of total lipid and TG concentrations.

Plasma biochemistry

Plasma alanine transaminase/glutamate pyruvate transaminase (ALT/GPT), TG, glycerol, creatine kinase (CK), non-esterified fatty acids (NEFA), glucagon, acetoacetate, fibroblast growth factor 21 (FGF21), glucose (Glc), β-hydroxybutyric acid (BHBA), and aspartate transaminase (AST) were photometrically analyzed (Abx Pentra 400; Horiba, Kyoto, Japan). Insulin (INS) and growth hormone (GH) concentrations in the blood samples were measured using radioimmunoassay kits (Beckman Coulter, Miami, FL, USA and Medilab, Malmö, Sweden, respectively), which have been validated for use in bovine plasma. The mean intra-assay coefficients of variation (CV) for duplicate samples were 3.9% and 3.5% for INS and GH, respectively. All inter-assay CVs were <10%.

Hepatic triglyceride content test

The liver tissue samples were tested in copper sulfate

solution and water with specific gravities of 1.025 and 1.055 (Herdt et al., 1983), respectively. Based on the buoyancy of the liver tissue in these liquids, the samples were classified as containing >35% lipid, >25% lipid, or <15% lipid (Herdt et al., 1983). Cows with TG contents >35% in the liver were grouped into the fatty liver group, and cows with TG contents <13% in the liver and with no clinical symptoms were grouped into the control group.

Sample preparation

Prior to ^{1}H NMR analysis, the plasma samples were thawed at room temperature. Deuterium oxide was added to each plasma sample (300 μL), which consisted of 150 μL buffer solution (pH 7.4, 0.2 mol/L Na_2HPO_4, and 0.2 mol/L NaH_2PO_4) and 150 μL sodium 3-trimethylsilyl-(2,2,3,3-D4) propionate (TSP; 1 mg/mL; Sigma-Aldrich, St. Louis, MO, USA). The plasma samples were centrifuged at 4°C (12,000 ×*g*) for 10 min. The aliquot of the resulting mixture (550 μL) was subsequently transferred to a 5 mm NMR tube.

Acquisition of ^{1}H NMR plasma spectra

Conventional ^{1}H NMR of the plasma samples were performed at 500 MHz on a Bruker Avance-500 spectrometer (Billerica, MA, USA) at 25°C. The spectra of the samples were recorded using the water-suppressed Carr–Purcell–Meiboom–Gill sequence with a spin–spin relaxation delay of 40 ms to suppress the broad signals of micromolecules. To provide sufficient data points for each resonance prior to Fourier transformation, the free induction decays were zero-filled to 64 K, and an exponential line broadening factor of 0.5 Hz was applied. All plasma ^{1}H NMR spectra were corrected for phase and baseline distortions using Bruker Topspin 3.0 software (Bruker GmbH, Karlsruhe, Germany) and were referenced to TSP (CH_3, δ 0.0).

Metabolite identification

The metabolites were assigned based on chemical shift and identified from a library of in-house pure compounds, Chenomx NMR suite (Version 7.5; Chenomx, Inc., Edmonton, Alberta, Canada), and database query (Madison: http://mmcd.nmrfam.wisc.edu/, HMDB: http://www.hmdb.ca/, etc.), and were identified by [1]H-^{1}H correlation spectroscopy and [1]H-^{13}C heteronuclear single quantum correlation. In order to enhance the information obtained from global metabonomic profiling of fatty liver, the Kyoto Encyclopedia of Genes and Genomes (http://www.genome.jp/kegg/) was utilized to map the marker metabolites with regards to the dairy cow metabolic pathways.

Data reduction of ^{1}H NMR data

Using the MestReNova software (Version 8.0.1;

Mestrelab Research SL, A Coruña, Spain), all ^{1}H NMR spectra were automatically reduced to American Standard Code for Information Interchange (ASCII) files. The ASCII files were imported into "R" (version 2.7.2; http://www.r-project.org) to eliminate phase and baseline variations. To reduce variability in peak positions, peak alignment scripts were built into the R software. The spectra (range of δ 0.5 to 4.3) were binned into integrated segments of equal width (δ 0.003) to assess differences in the concentrations between the samples. The aligned spectra were then normalized using probabilistic quotient normalization (Dieterle et al., 2006).

Multivariate analysis

Multivariate analysis was conducted on the ^{1}H NMR data, which included unsupervised principal component analysis (PCA) and supervised orthogonal projections to latent structures discriminant analysis (OPLS-DA).

First, an initial overview of the PCA analysis was used to decrease the dimensionality of the data and display the internal structure of the datasets in an unbiased way. Then, the OPLS-DA models were constructed to identify the marker metabolites between the different groups. The OPLS-DA model was generated using t[1]P and t[2]O, which represent the first principal component and the second orthogonal component, respectively. In the OPLS-DA model, the *X* variable and the *Y* variable represent the peak intensities in the ^{1}H NMR spectra and the predictive classifications, respectively. With a 10-fold cross-validation in the OPLS-DA models, Q^2 and R^2Y values were obtained, which represent the predictive ability of the model and the explained variance, respectively. Score plots were used to identify differential metabolites between the two groups and to combine the reliability and correlation from the OPLS-DA models.

Each point, the center of each ellipse, and the margin in the OPLS-DA score plots represent an individual sample, mean, and standard deviation (SD), respectively. Based on the cross-validated residuals (CV-ANOVA), the S-plot from the OPLS-DA analysis was used to indicate the contributions to clustering and to identify the significant metabolites between the two groups (Song et al., 2013). The p(corr)[1] axis and p[1] axis towards the predictive variation shown in the S-plot represent the correlation and magnitude of the spectral bins, respectively. The points in the S-plot represent the bins of the OPLS-DA. In the S-plot, the top or bottom points represent a stronger contribution to the class separation and more change in the variables compared with the middle points. The color-coded loading plots from the OPLS-DA analysis indicate changes in the metabolite between the two groups. In the color-coded loading plots, signals with a positive direction indicate a decreased metabolite level in the fatty liver group; in

contrast, signals with a negative direction indicate an increased metabolite level in the fatty liver group (Sun et al., 2014). The color of the coefficient plots represent the importance of the significant metabolites in explaining the scores. In the coefficient plots, red indicates a more significant contribution to the separation between the two groups, and the opposite is true of blue.

The biplot (correlation circle) obtained from the partial least squares discriminant analysis (PLS-DA) represents the biochemical parameters and the correlation of metabolites between the two groups. The *x*-axis, *y*-axis, and the concentric circles in the biplot represent the first and second components of the PLS-DA model and the explained variance, respectively (Song et al., 2013).

Univariate analysis

Statistical differences among groups in terms of clinical data, plasma biochemistry, and plasma enzymes data, and ^{1}H NMR spectra of potential biomarkers from the differential metabolites were calculated by one way of analysis of variance (ANOVA) using SPSS statistical software (Version 11.0; SPSS, Inc., Chicago, IL, USA). A p values of <0.05 were considered to be statistically significant. Data were expressed as the mean±SD.

Receiver operating characteristic (ROC) curves were constructed for the ^{1}H NMR spectra data of the identified metabolites using SPSS statistical software. In this study, ROC curves were used to test the diagnostic value of the potential biomarkers from the differential metabolites of the fatty liver. Typically, area under the curve values greater than 0.8 and larger positive likelihood ratio values, which were calculated from the ROC analysis, indicate excellent predictive ability (Zhang et al., 2013).

RESULTS

Liver evaluation and clinical information

The liver tissues from the 171 cows were tested with the liver TG content test method described in previous studies (Herdt et al., 1983). Thirty-two cows with fatty liver and 32 healthy cows were selected for this study, as shown in Table 1. The clinical data for the control and fatty liver groups revealed biochemical differences between the groups (Table

Table 1. Clinical data for the control (C) and fatty liver (F) groups

Parameters	C	F	p-values
Number	32	32	
Age (yr)	3.46±1.06	3.50±0.85	0.860
Parity	1.78±0.83	1.65±0.87	0.555
Days in milk	15.50±6.02	16.31±4.30	0.557
MY (kg/d)	30.75±3.70	28.32±4.73	0.030
BCS	3.16±0.32	2.88±0.34	0.001

MY, milk yield; BCS, body condition score; SD, standard deviation.
Data are expressed as the mean±SD.

1). There were no significant differences between the two groups in terms of age, parity, and days in milk (p>0.05). However, MY (p<0.05) and BCS (p<0.01) were significantly different between the two groups.

Plasma biochemistry analysis

Compared with the control group, the main differences in the fatty liver group included increased NEFA (p<0.001) and BHBA (p<0.001), and decreased CK (p<0.001), FGF21 (p<0.001), INS (p<0.01), Glc (p<0.01), TG (p<0.05) and AST (p<0.05) (Table 2).

^{1}H NMR spectra analysis

Figure 1 shows the representative ^{1}H NMR spectra (*δ* 0.5 to 4.3) of the plasma samples from the control and fatty liver groups, with the major metabolites labeled. The main differences in the fatty liver group compared with the control group were increased isobutyrate (IB), BHBA, acetone (ACTN), citrulline (Citn), and trimethylamine-*N*-oxide (TMAO) (p<0.001), valine (Val) and glycine (Gly) (p<0.01), and decreased alanine (Ala), glycerol, α-Glc, and β-Glc (p<0.001), asparagine (Asn) and γ-aminobutyric acid (GABA) (p<0.01), and creatinine (Cr) (p<0.05) (Table 3). A supervised OPLS-DA analysis was conducted to identify significant metabolite changes and to ascertain differences between the control and fatty liver groups (Table 3).

A PCA with pareto-scaled data was first conducted; however, the two groups were not well clustered (data not shown). Thus, an OPLS-DA model was constructed to identify the differences in the metabolites between the fatty

Table 2. Results of the identified plasma metabolites and plasma enzymes obtained from the photometric analysis

No.	Metabolites	C	F	p-values
1	ALT/GPT (U/L)	4.18±3.11	3.50±2.34	0.226
2	AST (U/L)	58.77±31.63	23.00±5.42	0.028
3	TG (mmol/L)	0.10±0.02	0.09±0.01	0.028
4	Glycerol (mg/dL)	33.14±15.58	34.27±15.32	0.428
5	CK (U/L)	1.48±0.76	0.97±0.86	<0.000
6	NEFA (mmol/L)	0.55±0.29	12.24±0.62	<0.000
7	GC (ng/L)	50.10±9.47	48.46±8.83	0.677
8	INS (μIU/mL)	6.97±1.00	6.19±1.06	0.004
9	ACAC (mg/dL)	2.88±0.46	3.00±1.13	0.934
10	GH (ng/mL)	5.63±1.20	5.33±1.25	0.678
11	FGF21 (pg/mL)	322.47±88.16	501.00±94.69	<0.000
12	Glc (mmol/L)	3.14±0.71	2.70±1.31	0.003
13	BHBA (mmol/L)	0.87±0.30	3.14±1.21	<0.000

C, control; F, fatty liver; ALT/GPT, alanine transaminase/glutamate pyruvate transaminase; TG, triglyceride; CK, creatine kinase; NEFA, non-esterified fatty acid; GC, glucagon; INS, insulin; ACAC, acetoacetate; GH, growth hormone; FGF21, fibroblast growth factor 21; Glc, glucose; BHBA, β-hydroxybutyric acid; AST, aspartate transaminase; SD, standard deviation.
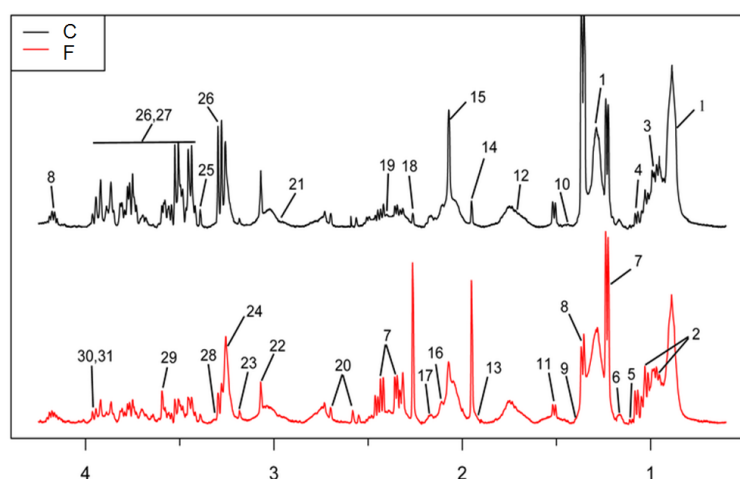Data are expressed as the mean±SD.

Figure 1. Typical ^{1}H nuclear magnetic resonance–metabolomics spectra of the plasma extracted from samples; the identified metabolites are labeled. "C" and "F" indicate the control and fatty liver groups, respectively. Metabolites: 1 low-density lipoprotein/very-low-density lipoprotein, 2 isoleucine, 3 leucine, 4 valine, 5 isobutyrate, 6 ethanol, 7 β-hydroxybutyric acid, 8 lactate, 9 threonine, 10 α-hydroxy-n-valerate, 11 alanine, 12 lysine, 13 gamma-aminobutyric acid, 14 acetate, 15 N-acetyl glycoprotein, 16 O-acetyl glycoprotein, 17 glutamate/glutamine, 18 acetone, 19 succinate, 20 citrate, 21 asparagine, 22 creatinine, 23 citrulline, 24 choline, 25 glycerol, 26 β-glucose, 27 α-glucose, 28 trimethylamine-*N*-oxide, 29 glycine, 30 betaine, and 31 creatine.

liver and control groups (Figure 2). The OPLS-DA score plot (Figure 2A) demonstrates an obvious separation between the fatty liver and control groups (p<0.05), with an R^2Y of 91.3% and a Q^2 of 80.1%.

The loadings S-plot was used to identify the variant spectral bins for the inter-class differences (Figure 2B). This plot is typically applied to identify metabolites, and to reduce the risk of false positives in the metabolite selection. It is also often used to visualize covariance p(1) (*x*-axis) and correlation p(corr) (*y*-axis), which are obtained from the OPLS-DA model (Song et al., 2013). In the S-plot, the lower left and the upper right quadrants exhibit positive and negative correlation and covariance, respectively. The significant metabolites in the lower left quadrant were increased in the fatty liver group; in contrast, the significant metabolites in the upper right quadrant were decreased in the fatty liver group. The further away from the center of the S-plot (Figure 2B), the more significant the contribution of the endogenous metabolites for clustering in the score plot. The S-plot illustrated that the metabolites that separated the two groups were primarily BHBA (δ 1.220 to 1.237), lipoprotein (δ 1.244 to 1.271), glutamine (Gln) and glutamate (Glu) (δ 2.255 to 2.266), and Glc (δ 3.296 to 3.422).

The color-coded corresponding coefficient plots of the OPLS-DA revealed additional detailed information regarding the metabolic differences between the fatty liver and healthy control groups (Figure 2C). The value of |r^2|, which represents the absolute correlation coefficient of each variable, displays the class separation of the two groups. In the color-coded loadings plot, red indicates a more significant contribution to the separation between the two

groups compared with blue (Zhang et al., 2013). The color-coded loading plots (Figure 2C) show a decrease in the levels of Ala, α-Glc, β-Glc, and GABA, and an increase in the levels of low-density lipoprotein/very-low-density lipoprotein, Val, BHBA, acetate, glycerol, and lactate in the fatty liver group compared with the control group.

Based on the results of the OPLS-DA S-plot (Figure 2B) and the color-coded loadings plot (Figure 2C), 31 metabolites were identified as potential metabolite biomarkers of fatty liver in cows. *T*-tests were used to calculate the p-values of the concentrations of the 31 metabolites between the two groups; the results are summarized in Table 3.

Correlations between the endogenous metabolites and the biochemical parameters

In Figure 3, the biplot of the PLS-DA model was based on all ^{1}H NMR and biochemical data, and was used to further investigate the correlations between metabolites and biochemical responses in the fatty liver and control groups. This plot was generated using the biochemical levels as *Y* variables and the metabolite contents as *X* variables ($R^2 = 0.81$, $Q^2 = 0.64$). The metabolites in the right quadrants are positively correlated with the fatty liver group, while the metabolites in the left quadrants are negatively correlated with the fatty liver group. As shown in Figure 3, the metabolites glycerol and Glc, which were detected by biochemical methods or NMR, are both positively correlated with the fatty liver group, which demonstrates the reliability of our results. In addition, Figure 3 shows that Glc and INS are negatively correlated with BHBA, acetate, ACTN, and citrate; Glu and Gln are negatively correlated

Table 3. Results from the ^{1}H nuclear magnetic resonance spectra analysis and the classification of the identified metabolites

No.	Metabolite	Chemical shift (ppm)	C	F	p-value	LR+	AUC
1	LDL/VLDL	0.866-0.920, 1.250-1.275, 1.30-1.35, 2.0-2.05, 3.225-3.262	3,690.40±541.84	3744.73±756.84	0.8374	0.9990	0.5010
2	Isoleucine	0.925-0.960, 1.035-1.060	492.13±62.93	487.24±60.05	0.8374	1.2903	0.5020
3	Leucine	0.965-0.993, 1.825-1.850	377.51±47.67	380.06±66.36	0.8804	4.1290	0.4829
4	Valine	1.010-1.031, 1.065-1.085	267.26±35.88	303.49±45.74	0.0025	8.2581	0.7077
5	Isobutyrate	1.090-1.115	4.94±0.81	14.84±6.12	<0.0000	12.3871	0.8942
6	Ethanol	1.180-1.220,	302.09±260.78	232.01±156.45	0.4483	1.8433	0.5685
7	BHBA	1.225-1.238, 2.305-2.360, 2.398-2.430, 4.164-4.205	657.14±131.87	1,351.49±383.50	<0.0000	27.8710	0.9808
8	Lactate	1.350-1.375, 4.155-4.180	580.43±276.34	549.51±157.87	0.9613	1.1470	0.4929
9	Threonine	1.378-1.415, 3.63-3.65	57.05±22.71	77.72±41.70	0.0787	5.6774	0.6492
10	α-Hydroxy-n-valerate	1.420-1.445	11.15±0.27	7.60±0.87	0.0965	0.9677	0.3589
11	Alanine	1.500-1.525	101.68±18.63	70.67±15.15	<0.0000	0.9677	0.1008
12	Lysine	1.72-1.76	186.61±17.31	195.30±22.26	0.1499	5.1613	0.6472
13	GABA	1.905-1.942, 2.278-2.302	107.12±18.03	103.67±26.57	0.0035	4.1290	0.4103
14	Acetate	1.945-1.952	159.05±76.30	194.80±74.44	0.0733	3.6129	0.6532
15	NAGP	2.068-2.076	135.90±29.03	149.40±41.86	0.2656	5.1613	0.5978
16	OAGP	2.100-2.120	103.99±17.85	103.87±15.67	0.9773	1.5484	0.5101
17	Glutamate/Glutamine	2.150-2.200, 2.475-2.525	131.39±17.85	120.51±34.17	0.2642	3.0968	0.3861
18	Acetone	2.255-2.275	53.94±27.96	452.42±194.79	<0.0000	28.9032	0.9798
19	Succinate	2.375-2.4	67.37±4.07	70.57±10.90	0.2090	13.4194	0.6361
20	Citrate	2.550-2.554, 2.690-2.720	65.22±12.78	57.85±12.92	0.0565	1.0323	0.3478
21	Asparagine	2.975-3.020	134.27±12.90	120.02±19.44	0.0031	1.0323	0.2692
22	Creatinine	3.065-3.075	93.80±11.94	87.32±13.43	0.0362	2.0645	0.3236
23	Citrulline	3.14-3.195	83.69±20.13	104.15±226.59	<0.0000	2.0645	0.1421
24	Choline	3.225-3.265	594.69±86.51	568.84±10.28	0.3987	2.0645	0.4073
25	Glycerol	3.59-3.70	33.70±7.91	22.62±7.02	<0.0000	0.9677	0.1512
26	β-Glucose	3.275-3.300, 3.415-3.47, 3.478-3.530, 3.54-3.585, 3.73-3.825	1,387.69±205.07	1,026.91±398.55	<0.0000	1.0323	0.0857
27	α-Glucose	3.85-3.890, 3.927-3.975, 3.415-3.47, 3.478-3.530, 3.54-3.585, 3.73-3.825	1,363.10±206.03	1,019.59±374.66	<0.0000	0.9677	0.0837
28	TMAO	3.305-3.325	5.09±0.27	14.84±7.83	<0.0000	14.4516	0.8266
29	Glycine	3.585-3.60	58.10±11.59	67.84±8.96	0.0011	3.0968	0.7560
30	Betaine	3.950-3.970	35.09±6.11	33.86±4.28	0.4482	1.1561	0.4103
31	Creatine	3.970-3.985	8.02±3.55	7.66±2.39	0.7589	1.2496	0.5071

C, control; F, fatty liver; LR+, a positive likelihood ratio; AUC, area under the curve; LDL/VLDL, low-density lipoprotein/very-low-density lipoprotein; BHBA, β-hydroxybutyric acid; GABA, γ-aminobutyric acid; NAGP, N-acetyl glycoprotein; OAGP, O-acetyl glycoprotein; TMAO, trimethylamine-*N*-oxide; SD, standard deviation.
Data of peak intensity are expressed as the mean±SD.

with AST, ALT/GPT, and GH.

DISCUSSION

Many studies have demonstrated that metabolomics techniques are powerful tools for identifying metabolites from multiple biological samples with biochemical variation. In addition, we have used gas chromatography/mass spectrometry and NMR techniques to assess clinical and subclinical ketosis in dairy cattle and identified significant metabolites (Zhang et al., 2013; Sun et al., 2014). In the present study, ^{1}H NMR-based

metabolomics was used to identify plasma metabolites in dairy cows with fatty liver and controls. The results clearly indicate significant differences in the metabolite concentrations between the control cows and the cows with fatty liver. In this study, BHBA and ACTN were higher in the fatty liver group. Conversely, the plasma Glc levels in the fatty liver group were lower compared with the control group. These results (Table 3) are consistent with the experimental data shown in Table 2.

Previous studies have showed that the lipid content in the liver of dairy cows is closely related to liver specific gravity (Herdt et al., 1983). To estimate the liver lipid
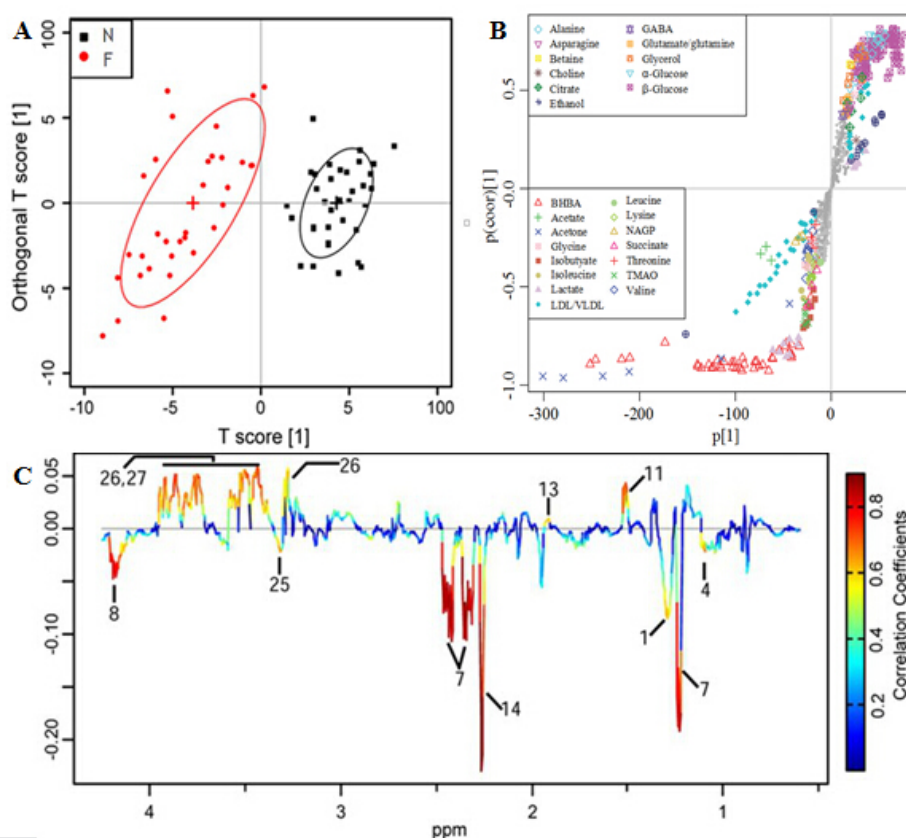
Figure 2. Orthogonal projections to latent structures discriminant analysis (OPLS-DA) model with the metabolites labeled in Figure 1. (A) Score plot obtained from the OPLS-DA analysis of the control group (■) and the fatty liver group (●) (n = 32); (B) S-plot obtained from the OPLS-DA analysis of the control and fatty liver groups corresponding to the score plot (Figure 2A); (C) color-coded loadings plot from the OPLS-DA analysis illustrating the metabolite components that differ between the two groups. Red indicates the greatest difference, with statistical significance; blue indicates the smallest difference, with no significant difference between the groups. Metabolites: 1 low-density lipoprotein/very-low-density lipoprotein, 4 valine, 7 β-hydroxybutyric acid, 8 lactate, 11 alanine, 13 γ-aminobutyric acid, 14 acetate, 25 glycerol, 26 β-glucose, and 27 α-glucose.

content of dairy cows, this observation was used as the basis for a clinical test. An increase in liver fat concentration during the peripartum period is extremely common in dairy cows and, to some degree, is likely normal. To obtain accurate biomarkers, cows with TG contents between 13% and 34% in the liver were not included in the study. In this study, cows with TG contents >35% in the liver were included in the fatty liver group, and cows with no clinical signs and TG contents <13% in the liver were included in the control group.

As a result of high milk production, high-yielding dairy cows typically experience NEB during early lactation. Dairy cows with NEB exhibit increased gluconeogenesis and mobilization of body TG and protein (Sun et al., 2014). Compared with monogastric animals, Glc regulation is very complicated in ruminant animals. Due to the lack of carbohydrates in the body and/or increasing energy requirements, ruminant animals predominately depend on non-carbohydrate compounds to meet their energy demands via gluconeogenesis (Laffel, 1999). Therefore, the primary changes include high ketone bodies, glucopenia, and high

TG in the blood (Xu et al., 2008). In this study, the high levels of IB, BHBA, and ACTN and the low levels of Ala, Asn, Glc, and Cr in the fatty liver group were similar to those found in previous research (Xu et al., 2008).

During metabolism, chain amino acids such as Val, leucine (Leu), and isoleucine (Ile) produce Ala. Blood Ala is one of the primary materials required for the synthesis of Glc through the gluconeogenesis pathway. The concentration of Ala in blood has been found to be highly correlated with many metabolic pathways, including gluconeogenesis, glycolysis, and the tricarboxylic acid cycle (TCA cycle) (Mukherjee et al., 2010). In energy-deficient states, Ala enters the TCA cycle to generate Glc for energy, and can also give rise to Glc via the Ala cycle. In the current experiment, Ala decreased in the fatty liver group compared with the control group. This result implies that low concentrations of blood Ala are closely associated with fatty liver; a similar result was reported in previous research (Mukherjee et al., 2010).

In the current experiment, the levels of blood Asn were lower in the cows with fatty liver than in the control cows,
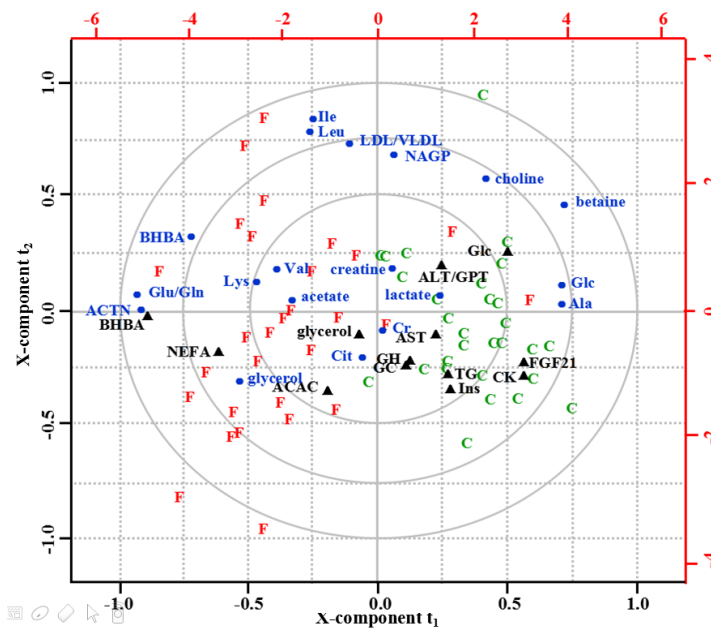
Figure 3. The biplot showing the correlation between the endogenous metabolites and biochemical parameters. "C" and "F" indicate the control and fatty liver groups, respectively. ALT/GPT, alanine transaminase/glutamate pyruvate transaminase; TG, 'triglyceride; CK, creatine kinase; NEFA, non-esterified fatty acid; GC, glucagon; INS, insulin; ACAC, acetoacetate; GH, growth hormone; FGF21, fibroblast growth factor 21; Glc, glucose; BHBA, β-hydroxybutyric acid; AST, aspartate transa-minase; LDL/VLDL, low-density lipoprotein/very-low-density lipoprotein; Ile, isoleucine; Leu, leucine; Val, valine; Lys, lysine; ACTN, acetone; Cr, creatinine; Ala, alanine; Cit, citrate; Glu/Gln, glutamate/glutamine.

which implies that, as a glucogenic amino acid, Asn can be metabolized by gluconeogenesis or the TCA cycle. Moreover, it also plays an important role in glycosylation, which is closely related to protein structure and function (Patterson, 2005).

In this study, the concentration of blood Cr was significantly lower in the fatty liver group than in the control group. Previous research has demonstrated that the concentration of Cr in the blood or urine provides an accurate measure of renal function (Shemesh et al., 1985). Another study demonstrated a relationship between low levels of serum Cr and increased risk for the development of type 2 diabetes (Harita et al., 2009). These findings imply that the levels of Cr typically decrease due to weakened aerobic metabolism during NEB, which is an important mesostate of the TCA cycle.

As an important component of bile acids, Gly is necessary for dietary fat digestion and long-chain fatty acid absorption. Furthermore, Gly has been used to treat metabolic disorders such as obesity, ischemia–reperfusion injuries, cardiovascular disease, and diabetes (Wu et al., 2012). In the current study, the concentrations of Gly were higher in the fatty liver group than in the control group, which indicates that Gly was used to correct lipid metabolic disorder during the functional compensatory period.

A previous study has demonstrated that Val can regulate lipid metabolism and increase fat loss via increased energy expenditure (Du et al., 2012). In animal models, Val induces

non-alcoholic fatty liver disease via oxidative stress. Another study indicated that a low Val supply could represent a limiting factor for milk protein synthesis (Haque et al., 2013). The results of the present study indicate that the levels of Asn were higher in the cows with fatty liver than in the control group, suggesting that Val can reverse the liver damage caused by lipid metabolic disturbance.

Our results suggest an increased demand for energy via a potential increase in the precursors for the TCA cycle and gluconeogenesis compared with dairy cows in lactation (Moyes et al., 2013). A series of metabolic abnormalities were associated with fatty liver, which could be considered as diagnostic biomarkers.

Liver disease is typically caused by metabolic abnormalities. Liver damage can also result from characteristic changes in plasma amino acid levels. Some plasma amino acids are highly related to liver damage, with clear concentration changes after liver damage (Ning et al., 1967). As an inhibitory neurotransmitter, deficiency in GABA may cause decreased attention span, memory alterations, mood changes, and drowsiness, and these symptoms are consistent with the clinical symptoms of cows with fatty liver (Xu et al., 2008; Mukherjee et al., 2010). Another study indicated that GABA in cows can promote gastric juice production, thus improving growth rate and feed intake (Mukherjee et al., 2008). The fatty liver cow group showed significant deficiency of plasma GABA compared with the control group. The results of the present

study indicate that GABA acts as an inhibitor of fatty liver and obesity by activating hepatic function and avoiding NEB. We suggest that the downstream events of GABA deficiency may be important in the initiation of fatty liver disease.

Previous studies have shown increased level of TMAO, which acts as a chemical toxin, inducing liver damage in a mouse model accompanied by the suppression of glycolysis, stimulation of fatty acid oxidation, and increased levels of oxidative stress (Zhao et al., 2011). A study published in 2013 indicated that TMAO is related to cholesterol metabolism in artery walls, intestines, and the liver. In artery walls, TMAO can reduce cholesterol removal and increase cholesterol deposition (Koeth et al., 2013).

In the urea cycle, Citn is produced from ornithine and carbamoyl phosphate. A high plasma Citn level is related to several human liver-damage diseases, such as liver fibrosis and type I/II citrullinemia (Faghfoury et al., 2011; Takahashi et al., 2012). In addition, the circulating Citn concentration is, in humans, a biomarker of intestinal functionality (Crenn et al., 2003). In the current study, the level of Citn was lower in the plasma of cows with fatty liver than in healthy cows, which suggests that fatty liver is related to liver-damage diseases in cows.

Fatty liver in mice is a multi-factorial disease in which abnormal TG accumulation in hepatocytes can result from a number of distinct alterations. It has recently been *reported* that synthesis of TGs requires esterification of one glycerol molecule with three fatty acids, and aquaporin-9 has been

found to play a major role in glycerol import by mouse hepatocytes (Gena et al., 2013).

Glycerol, TMAO, and Citn have important effects on liver damage and lipid imbalance. To our knowledge, these metabolites have not been studied in fatty liver in cows. Additional research is required to explain the specific mechanisms involved, and disease diagnostic assays require more complex procedures.

Routine plasma biochemistry was performed for all dairy cows in this study. Several compounds, such as Glc, BHBA, CK, and NEFA, confirmed the hepatic TG content-based grouping. Most of the parameters, especially glycerol, TG, ALT/GPT, and AST, which are supposed to be closely related to fatty liver, failed to be effective biomarkers.

Metabolomics provides a new viewpoint and technology platform to assist in the early diagnosis and efficacy assessment of many diseases. The testing of entire datasets for metabolic features is critical for assessing the processes of fatty liver. ^{1}H NMR-based metabolomics is a novel method for detecting cows with fatty liver. In this study, plasma metabolic profiling and data analysis methods were used to predict the diagnosis of cows with and without fatty liver, with high specificity and sensitivity. The development of fatty liver involves disturbances in the metabolism of amino acids and fatty acids, as well as in gluconeogenesis (Figure 4). In the present study, the levels of 13 metabolites were significantly different between dairy cows with fatty liver and control cows. Our study demonstrates that these 13 metabolites can be used in future
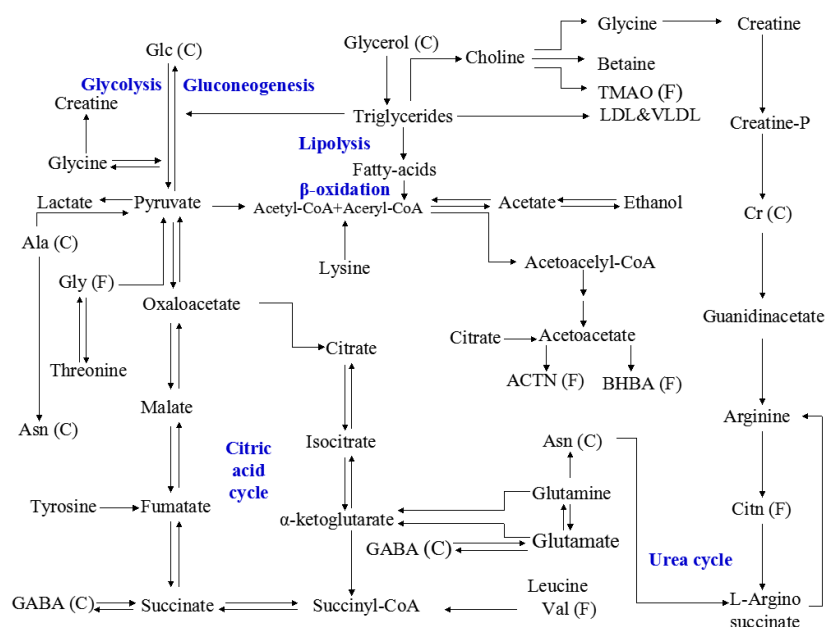

Figure 4. Schematic representation of the most relevant metabolic differences between the two groups. "F" and "C" indicate the metabolites that were higher or lower in the fatty liver group compared with the control group, respectively. Metabolites: LDL/VLDL, low-density lipoprotein/very-low-density lipoprotein; Ala, alanine; Asn, asparagine; Glc, glucose; BHBA, β-hydroxybutyric acid; Cr, creatinine; GABA, γ-aminobutyric acid; glycerol; ACTN, acetone; Citn, citrulline; Gly, glycine; IB, isobutyrate; TMAO, trimethylamine-*N*-oxide; Val, valine.

as potential diagnostic biomarkers for dairy cows with fatty liver. Previous studies have also identified the concentrations of BHBA, Citn, Ala, Ile, Leu, Gly, and Glc in cows blood as potential metabolite biomarkers (Zhang et al., 2013; Sun et al., 2014). Future studies should evaluate and optimize the diagnostic abilities of the 13 metabolites found in this study for fatty liver.

CONCLUSION

Through ^{1}H NMR detection and data analysis, 31 metabolites were identified between the fatty liver and control groups. The results demonstrate that the ^{1}H NMR technique combined with multivariate statistical analysis can be used to access the changes and progression of fatty liver and to discover potential biomarkers for this disease in cows. In future, changes in the potential metabolites and metabolic pathways could present new strategies for the diagnosis and prevention of fatty liver in dairy cows.

CONFLICT OF INTEREST

We certify that there is no conflict of interest with any financial organization regarding the material discussed in the manuscript.

ACKNOWLEDGMENTS

REFERENCES

Crenn, P., K. Vahedi, A. Lavergne-Slove, L. Cynober, C. Matuchansky, and B. Messing. 2003. Plasma citrulline: a marker of enterocyte mass in villous atrophy-associated small bowel disease. Gastroenterology 124:1210-1219.

Dieterle F., A. Ross, G. Schlotterbeck, and H. Senn. 2006. Probabilistic quotient normalization as robust method to account for dilution of complex biological mixtures. Application in 1H NMR metabonomics. Anal. Chem. 78: 4281-4290.

Du Y., Q. Meng, Q. Zhang, and F. Guo. 2012. Isoleucine or valine deprivation stimulates fat loss via increasing energy expenditure and regulating lipid metabolism in WAT. Amino Acids 43:725-734.

Faghfoury H., J. Baruteau, H. O. de Baulny, J. Häberle, and A. Schulze. 2011. Transient fulminant liver failure as an initial presentation in citrullinemia type I. Mol. Genet. Metab. 102: 413-417.

Gena, P., M. Mastrodonato, P. Portincasa, E. Fanelli, D. Mentino, A. Rodríguez, R. A. Marinelli, C. Brenner, G. Frühbeck, M. Svelto, and G. Calamita. 2013. Liver glycerol permeability and aquaporin-9 are dysregulated in a murine model of non-alcoholic fatty liver disease. PLoS One. 8:e78139.

Gonzalez, F. D., R. Muino, V. Pereira, R. Campos, and J. L. Benedito. 2011. Relationship among blood indicators of lipomobilization and hepatic function during early lactation in high-yielding dairy cows. J. Vet .Sci. 12:251-255.

Haque, M. N., H. Rulquin, and S. Lemosquet. 2013. Milk protein responses in dairy cows to changes in postruminal supplies of arginine, isoleucine, and valine. J. Dairy Sci. 96:420-430.

Harita, N., T. Hayashi, K. K. Sato, Y. Nakamura, T. Yoneda, G. Endo, and H. Kambe. 2009. Lower serum creatinine is a new risk factor of type 2 diabetes: the Kansai healthcare study. Diabetes Care 32:424-426.

Herdt, T. H., L. Goeders, J. S. Liesman, and R. S. Emery. 1983. Test for estimation of bovine hepatic lipid content. J. Am. Vet. Med. Assoc. 182:953-955.

Laffel, L. 1999. Ketone bodies: A review of physiology, pathophysiology and application of monitoring to diabetes. Diabetes Metab. Res. Rev. 15: 412–426.

Jorritsma R., H. Jorritsma, Y. H. Schukken, and G. H. Wentink. 2000. Relationships between fatty liver and fertility and some periparturient diseases in commercial Dutch dairy herds. Theriogenology 54:1065-1074.

Hayirli, A., R. R. Grummer, E. V. Nordheim, and P. M. Crump. 2002. Animal and dietary factors affecting feed intake during the prefresh transition period in Holsteins. J. Dairy Sci. 85:3430-3443.

Koeth, R. A., Z. Wang, B. S. Levison, J. A. Buffa, E. Org, B. T. Sheehy, E. B. Britt, X. Fu, Y. Wu, L. Li, J. D. Smith, J. A. DiDonato, J. Chen, H. Li, G. D. Wu, J. D. Lewis, M. Warrier, J. M. Brown, R. M. Krauss, W. H. Tang, F. D. Bushman, A. J. Lusis, and S. L. Hazen. 2013. Intestinal microbiota metabolism of L-carnitine, a nutrient in red meat, promotes atherosclerosis. Nat. Med. 19:576-585.

Moyes, K. M., E. Bendixen, M. C. Codrea, and K. L. Ingvartsen. 2013. Identification of hepatic biomarkers for physiological imbalance of dairy cows in early and mid lactation using proteomic technology. J. Dairy Sci. 96:3599-3610.

Mukherjee, S., S. K. Das, K. Vaidyanathan, and D. M. Vasudevan. 2008. Consequences of alcohol consumption on neurotransmitters -An overview. Curr. Neurovascular Res. 5:266-272.

Mukherjee, S., K. Vaidyanathan, D. M. Vasudevan, and S. K. Das. 2010. Role of plasma amino acids and gaba in alcoholic and non-alcoholic fatty liver disease-a pilot study. Indian J. Clin. Biochem. 25:37-42.

Ning, M., L. M. Lowenstein, and C. S. Davidson. 1967. Serum amino acid concentrations in alcoholic hepatitis. J. Lab. Clin. Med. 70:554-562.

Oikawa, S., Y. Mizunuma, Y. Iwasaki, and M. Tharwat. 2010. Changes of very low-density lipoprotein concentration in hepatic blood from cows with fasting-induced hepatic lipidosis. Can. J. Vet. Res. 74:317-320.

Patterson, M. C. 2005. Metabolic mimics: The disorders of N-linked glycosylation. Semin. Pediatr. Neurol. 12:144-151.

Sejersen, H., M. T. Sørensen, T. Larsen, E. Bendixen, and K. L. Ingvartsen. 2012. Liver protein expression in dairy cows with high liver triglycerides in early lactation. J. Dairy Sci. 95: 2409-2421.

Shemesh, O., H. Golbetz, J. P. Kriss, and B. D. Myers. 1985. Limitations of creatinine as a filtration marker in glomerulopathic patients. Kidney Int. 28:830-838.

Smith, T. R., A. R. Hippen, D. C. Beitz, and J. W. Young. 1997. Metabolic characteristics of induced ketosis in normal and obese dairy cows. J. Dairy Sci. 80:1569-1581.

Song, X. F., J. S. Wang, P. R. Wang, N. Tian, M. H. Yang, and L. Y. Kong. 2013. 1H NMR-based metabolomics approach to evaluate the effect of Xue-Fu-Zhu-Yu decoction on hyperlipidemia rats induced by high-fat diet. J. Pharm. Biomed. Anal. 78:202-210.

Sun, L. W., H. Y. Zhang, L. Wu, S. Shu, C. Xia, C. Xu, and J. S. Zheng. 2014. 1H-Nuclear magnetic resonance-based plasma metabolic profiling of dairy cows with clinical and subclinical ketosis. J. Dairy Sci. 97:1552-1562.

Takahashi, Y., S. Koyama, H. Tanaka, S. Arawaka, M. Wada, T. Kawanami, H. Haga, H. Watanabe, K. Toyota, C. Numakura, K. Hayasaka, and T. Kato. 2012. An elderly Japanese patient with adult-onset type II citrullinemia with a novel D493G mutation in the SLC25A13 gene. Intern. Med. 51:2131-2134.

Wildman, E. E., G. M. Jones, P. E. Wagner, R. L. Boman, H. F. Troutt Jr, and T. N. Lesch. 1982. A dairy cow body condition scoring system and its relationship to selected production characteristics. J. Dairy Sci. 65:495-501.

Wu, G., B. Imhoff-Kunsch, and A. W. Girard. 2012. Biological mechanisms for nutritional regulation of maternal health and fetal development. Paediatr. Perinat. Epidemiol. 26:4-26.

Xu, C., Z. Wang, G. W. Liu, X. B. Li, G. H. Xie, C. Xia, and H. Y. Zhang. 2008. Metabolic characteristic of the liver of dairy cows during ketosis based on comparative proteomics. Asian Australas. J. Anim. Sci. 21:1003-1010.

Zhang, H. Y., L. Wu, C. Xu, C. Xia, L. W. Sun, and S. Shu. 2013. Plasma metabolomic profiling of dairy cows affected with ketosis using gas chromatography/mass spectrometry. BMC Vet. Res. 9:186.

Zhao, X. J., C. Huang, H. Lei, X. Nie, H. Tang, and Y. Wang. 2011. Dynamic metabolic response of mice to acute mequindox exposure. J. Proteome Res. 10:5183-5190.